DEMONSTRATION OF FRESNEL INTERFERENCE BY MEANS OF A RIPPLE TANK

Thesis for the Degree of M. S.
MICHIGAN STATE UNIVERSITY
Claude M. Watson
1958

DEMONSTRATION OF FRESNEL INTERFERENCE BY MEANS OF A RIPPLE TANK

By

Claude M. Watson

AN ABSTRACT

Submitted to the College of Science and Arts of
Michigan State University of Agriculture and
Applied Science in partial fulfillment of
the requirements for the degree of

MASTER OF SCIENCE

Department of Physics

1958

Approved E. A. Hiedemann

ABSTRACT

The surface wave analogy of the diffraction of light by a slit and by a grating was used to show details of these phenomena which are unobservable in optics. Details a few wave lengths from the source (corresponding to a slit in optics) were shown and compared with the pictures of the corresponding analogy of a long, thin ultrasonic transducer. Also, the alternation of phase and amplitude modulation of the wave front in the Fresnel region of a grating, the increasing complexity of the patterns with increasing D/λ, and the similarity between the patterns produced by amplitude gratings and phase gratings were shown.

DEMONSTRATION OF FRESNEL INTERFERENCE BY MEANS OF A RIPPLE TANK

By

Claude M. Watson

A THESIS

Submitted to the College of Science and Arts of
Michigan State University of Agriculture and
Applied Science in partial fulfillment of
the requirements for the degree of

MASTER OF SCIENCE

Department of Physics

1958

ACKNOWLEDGEMENT

The author wishes to express his sincere appreciation to Dr. E. A. Hiedemann, who suggested the project and has given constant and helpful guidance through its development. He is also greatly indebted to Dr. M. A. Breazeale for his generous help and for his assistance with translations, upon which much of this study is based.

TABLE OF CONTENTS

TABLE OF FIGURES.

TABLE OF FIGURES (Cont.)

I. INTRODUCTION

Ripple tanks are widely used for demonstrating the characteristic phenomena of wave propagation, such as reflection, refraction, diffraction and interference. For lecture demonstrations one usually uses low frequency gravity waves on a water surface. The velocity of the gravity waves depends on the depth of the water below the surface: this fact allows one to demonstrate refraction. The low frequency necessitates the use of rather large troughs: 75 cm by 75 cm is the size used by R. W. Pohl[1]. For special studies, more elaborate types of ripple tanks have been described very early. Lord Rayleigh[2] studied surface tension prior to 1890 using capillary waves and a stroboscopic arrangement. J. H. Vincent[3,4,5] worked in mercury before the turn of the century, using an instantaneous spark for illumination and photographing the results. Out of the large number of more modern papers on ripple tanks, those presented by J. Baurand[6,7,8], H. Bondy[9], O. Brandt and H. Freund[10], A. H. Davis[11,12], W. R. Dean[13], G. Kreisel[14], M. S. Longuet-Higgins[15,16], J. Larras and J. Laurent[17], R. Mercier[18], E. Tyler[19], J. S. van Wieringen[20], and Yamasaki[21] are mentioned here as they contain interesting special techniques, experimental results or theoretical considerations.

In using a ripple tank, since the method is an analogy, there are several factors to consider. For example, one must consider the limitations on the analogy, the nature of the motion, and how the meniscus, contamination of the surface, and viscous damping affect this motion.

It is obvious that analogy between surface, sound and electromagnetic waves can be expected for all phenomena characteristic for every type of wave motion. For special types of waves, certain phenomena may occur to which there do not exist analogies in other types of waves. F. Ursell[22] describes, as an example, the trapping modes which are characteristic for the theory of surface waves, but do not occur in sound. The experimental observations have confirmed the analogy for the phenomena of reflection, refraction, diffraction and interference. However, one investigator, M. Bouasse[23], concluded from an extended study of the diffraction of capillary waves, that the Huygens' principle had no validity for surface waves. This statement was in direct contradiction to the results of E. Grossmann and E. Hiedemann[24], who had found that the diffraction of capillary waves by a slit revealed even the finer details of the interference pattern calculated from classical diffraction theory. The interference phenomena of capillary waves studied in this thesis give a further illustration of the complete analogy with the effects observed with electromagnetic or ultrasonic waves.

The velocity (v) of the surface wave is given by the relationship:

$$V^2 = f^2 \lambda^2 = \left(\frac{g\lambda}{2\pi} + \frac{2\pi\sigma}{\lambda\rho}\right) \tanh \frac{2\pi h}{\lambda} \qquad (1)$$

where f is frequency, λ is wave length, g is acceleration of gravity, σ is surface tension, ρ is density and h is the height of the liquid. For depths greater than $\lambda/2$, the hyperbolic tangent approaches one, so the expression reduces to the terms in the brackets. Numerical values of the velocity can be seen from the plot of velocity versus wave length in Figure 1. The curves are for water, clean mercury and dirty mercury. The value of λ for minimum velocity is given by

$$\lambda_{min} = \sqrt{\frac{4\pi^2\sigma}{g\rho}} \qquad (2)$$

This minimum for the three curves plotted is:

	λ_m	f_m	v_m
Water	1.73 cm.	13.4 cps	23.2 cm/sec
Clean Hg	1.29 cm.	15.7 cps	19.9 cm/sec
Dirty Hg	.94 cm.	18.3 cps	17.2 cm/sec

This minimum value is the dividing line between two classes of waves. For large wave lengths, the term $\frac{g\lambda}{2\pi}$ dominates. This is the region to the right of the minimum value in the plot. The waves here are commonly called gravity waves since gravity dominates. In this region one finds that the depth of the liquid is important in determining the wave length. This allows one, for

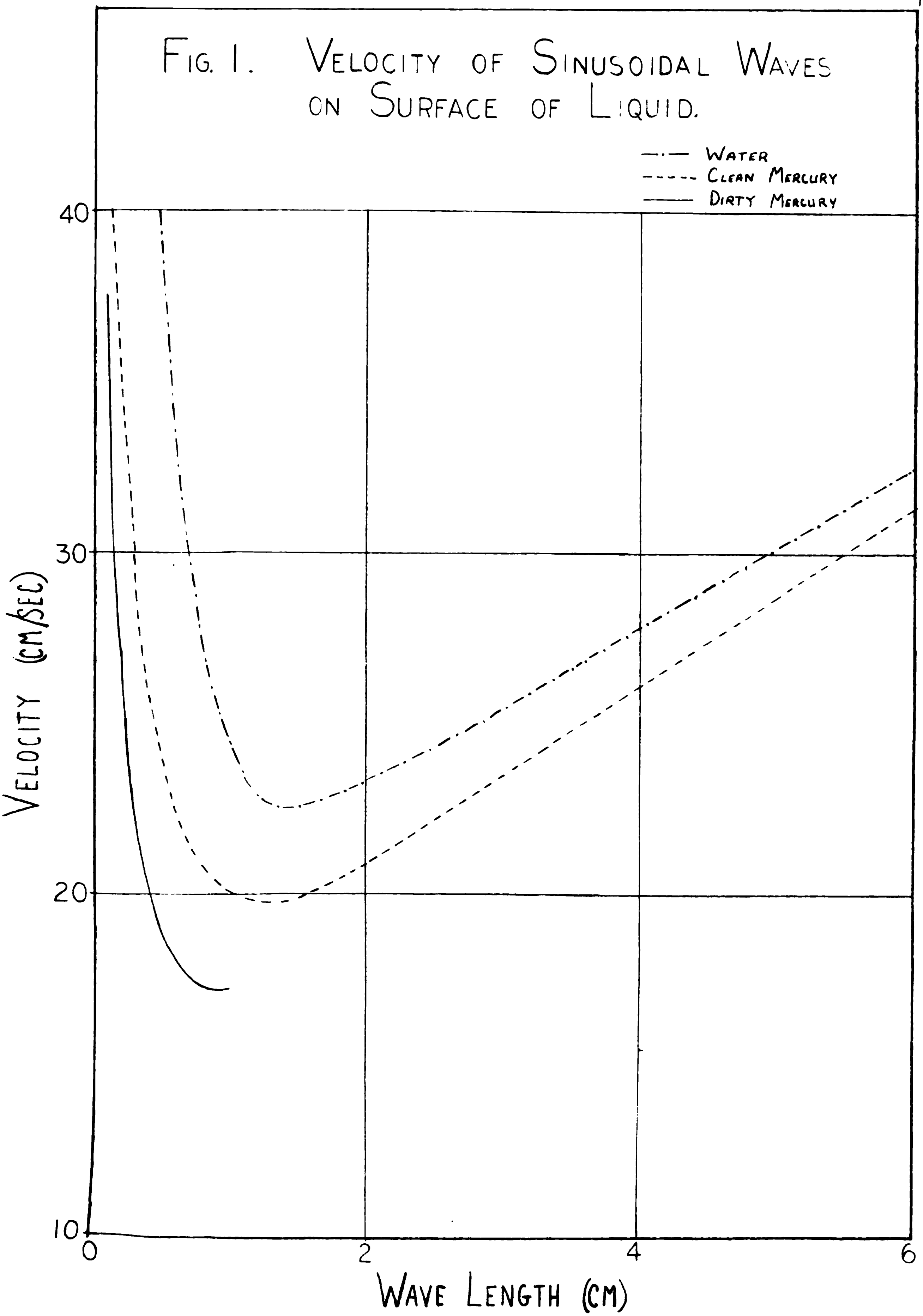
Fig. 1. Velocity of Sinusoidal Waves on Surface of Liquid.
Water
Clean Mercury
Dirty Mercury
Velocity (cm/sec)
Wave Length (cm)
10
20
30
40
0
2
4
6

example, to study refraction, since a variation in depth changes the velocity. Therefore, by putting a flat piece of solid in the shape of the lens on the bottom of the trough, one obtains an area of different refractive index in the form of a lens. For small wave lengths, the curve is to the left of the minimum value and the term $\frac{2\pi\sigma}{\lambda\rho}$ dominates. This is the region of capillary waves and is well suited to the study of diffraction. This region is particularly desirable because the absorption is greater, and, therefore, small tanks can be used. Also, with small wave length, many waves can be shown in a small space.

It is well known that contamination of the surface does affect the surface tension. Since surface tension does enter into the equation that is dominant for capillary waves, the velocity and wave length are changed for a given frequency. This change in wave length is immaterial, since the analogies still hold, but the viscous damping increases and the contamination usually shows up in photographs. In the case of mercury, the surface tension changes from 530 cgs units for clean mercury to 300 cgs units for dirty mercury. A thin film forms after a short exposure to air[25]. This film may be skimmed off frequently by drawing a plastic straight edge across the surface. Scum will adhere to the straight edge and the sides of the trough, presenting a clean surface again. In the case of water, fresh water is always available, so a clean surface is easier to obtain.

The viscous damping not due to changes in the surface is a more important consideration. Davis[12] has shown that the effect of viscosity on harmonic surface waves is similar to that on sound. This property is desirable in the analogy to sound, such as in the part of the demonstration dealing with beam patterns from a transducer. In the analogy comparing light and sound in this paper, it is important to have a large area relatively free from damping.

Lamb[26] has shown that for a depth of liquid greater than half a wave length, the velocity is unaltered by viscosity (ν), and the modulus of decay (τ) is given by:

$$\tau = \frac{1}{2\nu k^2} \qquad k = \frac{2\pi}{\lambda}$$

Expressing τ in terms of λ for water and mercury, $\tau_{water} \propto \lambda^2$ seconds and $\tau_{Hg} \propto 10\lambda^2$; or for the same amount of damping, a wave length in mercury can be one-third that of water[6]. Thus, for an extended field, mercury would seem to be favored slightly when using high frequencies.

II. EXPERIMENTAL APPARATUS

The optical set-up was designed to project parallel light on the surface of a mercury pool and to project an image of the surface wave on a screen or into a camera.

In Figure 2, light from the source O is focused by lens F_1 on a circular aperture S_1. Light from S_1 passes through a green filter F and is focused on the barrier B by lens F_2. The modulated light leaving this point is rendered parallel by the lens L_3, and is reflected to the mercury surface by the mirror M_1. Light reflected from the mercury surface is reflected again by mirror M_2. This mirror is placed as close as possible to M_1 to reduce distortion of the image by keeping the angle between incident and reflected light small and by keeping the incident angle nearly normal to the surface. An image of the surface is projected by lens L_4 on the camera or screen. The camera used was an Exacta V, which has a focal plane shutter, thus permitting the removal of the lens.

In order to observe traveling waves in a stationary position, it is necessary to provide stroboscopic illumination. It is possible to obtain stroboscopic illumination by using a mercury vapor lamp which is modulated at 120 cycles by the alternating line current and exciting the dipper on the mercury surface at the same frequency. Although this procedure in this case was extremely simple

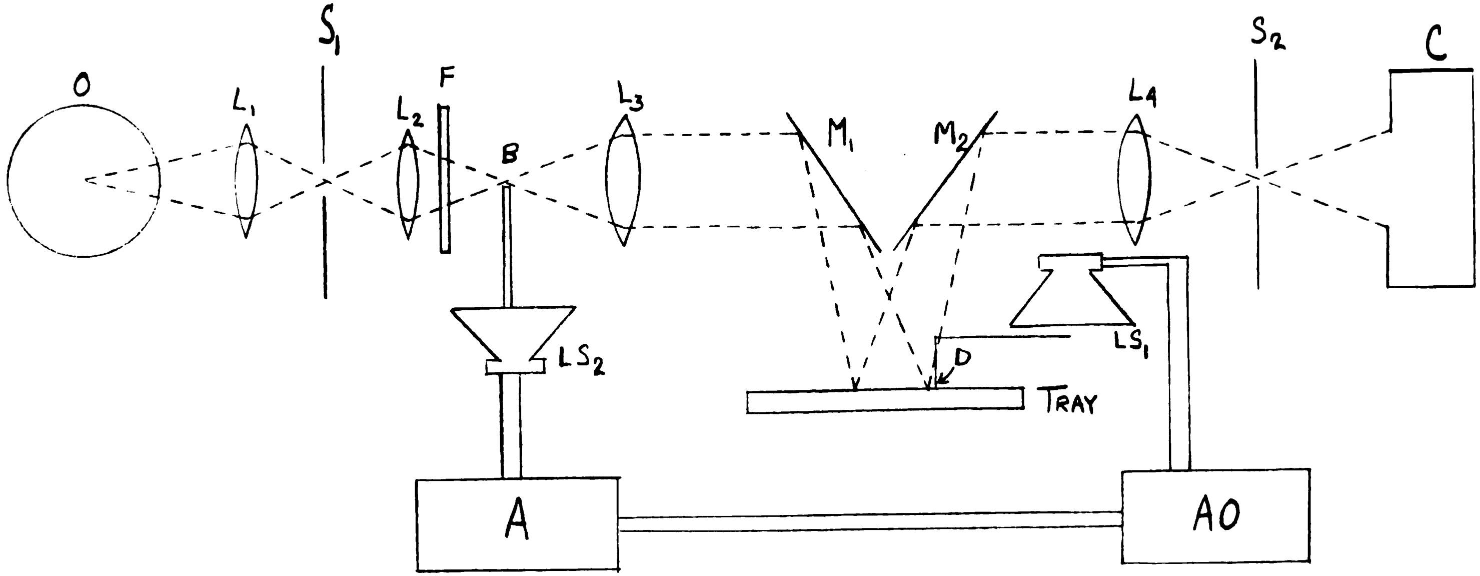

O	Projection lamp	L_1	Lens
S_1	Adjustable circular aperture.	L_2	Lens
S_2	Adjustable slit	L_3	Lens
F	Yellow filter	L_4	Lens
LS_1	Loud speaker strobe	A	Amplifier
LS_2	Loud speaker driver	AO	Audio Oscillator
M_1, M_2	Plane mirrors	C	Camera

Fig. 2. Components of Optical System.

it was abandoned because it excluded greater variations in the experimental conditions. The use of a special stroboscope was found to be much more satisfactory. This stroboscope was made by interrupting the light periodically by a barrier attached to the cone of a loud speaker. The speaker is excited by a signal from the same source as the dipper in the mercury. A continuous light source is obtained by using an incandescent lamp of such a type that the light is not modulated appreciably by the alternation of the line current.

The electrical system consisted of a Hewlett Packard audio oscillator, model 200C (AO in Figure 1). The output was connected directly to the loud speaker LS_1 driving the dipper (D). The signal was also connected to a Knight audio amplifier, thus providing a means of controlling the amplitude of vibration of the loud speaker LS_2, used to strobe the light. The loud speaker LS_1, used to drive the dippers, was a very ruggedly constructed surplus U. S. Coast Guard loud speaker, type COR-63-D. A rod was bolted to the voice coil in such a manner that dippers could be plugged into the end. For loud speaker LS_2, a cone was removed from a five inch loud speaker and most of the frame was cut away in order to get the speaker as close to the light beam as possible. A small piece of wood, long enough to extend into the light path, was cemented to the voice coil of the speaker.

This loud speaker was mounted on a sliding track to permit moving the speaker into and out of the light path.

Dippers were of three main types. Those used to simulate transducer sources (Figure 3a) were made of celluloid. Three of these were used, of widths .5 cm, 1.5 cm and 2 cm. These were cemented to a stiff wire which plugged into LS_1. The dippers simulating amplitude grating (Figure 3b) were constructed by removing teeth from combs until the right "grating spacing" was obtained. The dippers simulating the phase gratings (Figures 3c and 3d) were constructed by running thin strips of metal through the gear cogs used for corrugating in a sheet metal shop. Various shapes, from a sine wave to a saw tooth, could be obtained by varying the types of gears and the pressure. Metal dippers used in mercury must be coated with lacquer to prevent amalgamation.

Final adjustments were made with the dipper vibrating in the mercury. The best adjustment is obtained with a symmetrical dipper, perfectly level, and just touching the surface of the mercury. Since this adjustment was so critical, the loud speaker was mounted on a stand with adjustable leveling screws in the three feet.

The stroboscope was easily adjusted by moving it into the light beam. Best contrast was obtained by moving it to the point where the light was almost extinguished.

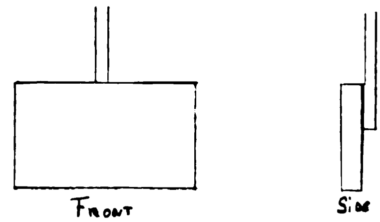

a. Celluloid Transducer

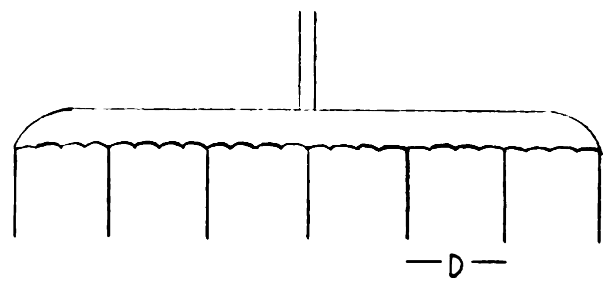

b. Amplitude Grating

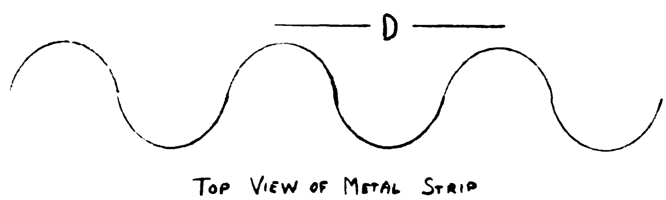

c. Sine Wave Phase Grating

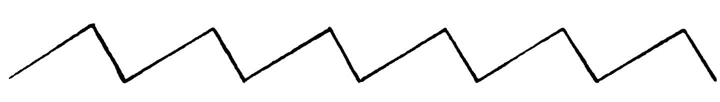

d. Saw-Tooth Phase Grating

Fig. 3. Dippers

In order to keep the mercury surface clean, occasional scumming is desirable. After each use the mercury was filtered.

III. BEAM PATTERNS

Fresnel diffraction may be observed near a slit illuminated by parallel light. The Fresnel region in a sound field near a vibrating quartz is analogous to the interference near a slit. Using the analogy discussed in the introduction, this Fresnel region can be produced by vibrating a thin, rigid dipper in water or in mercury. The width of this dipper is determined by the appropriate D/λ ratio for the analogous acoustical or optical case. Since λ changes with the frequency, a range of ratios D/λ is available for any particular width of the dipper. Although the nature of Fresnel diffraction has been thoroughly investigated, the ripple study is very useful because this ease in changing the ratio D/λ makes it possible to observe a wide range of D/λ readily, and even to demonstrate the change in pattern with D/λ to a large audience.

Fresnel diffraction for optics is well known and the intensity distribution in the Fresnel field can be calculated. However, only those structures in the optical interference pattern can be observed which are large compared with the wave length. The wave length of ultrasonic or of capillary waves is very large compared with the wave length of light. Therefore, even the finest details of an interference pattern produced by ultrasonic or capillary waves should be observable by

optical methods.

Early investigators attempted to determine experimentally the ultrasonic intensity pattern in front of a slit or transducer. Placing a measuring device in the field disturbs the field, however. Boyle, Lehmann and Reid[27] observed how small particles were driven by the radiation pressure in the sound beam and collected at points of minimum energy. This method allows one to find the direction of the main lobes of a beam pattern, but gives no finer details.

The development of optical techniques for the study of sound waves permitted the observation of waves without disturbing them. Hiedemann and Osterhammel[28,29], with these techniques, used long thin quartzes with light passing along the longest dimension. The resulting cylindrical symmetry enabled them to photograph sound intensity distributions which could be compared directly with light intensity distributions behind slits having the same ratios of D/λ. The symmetry inherent in surface waves makes it possible for one to make the same observations and analogies as did Hiedemann and Osterhammel. Some of their experimental results are illustrated in Figures 4, 5 and 6. Details of the waves themselves are shown in the stroboscopic pictures, Figures 4a and 5. The complete pattern of the beam can best be seen in Figure 4b, which has the same D/λ used

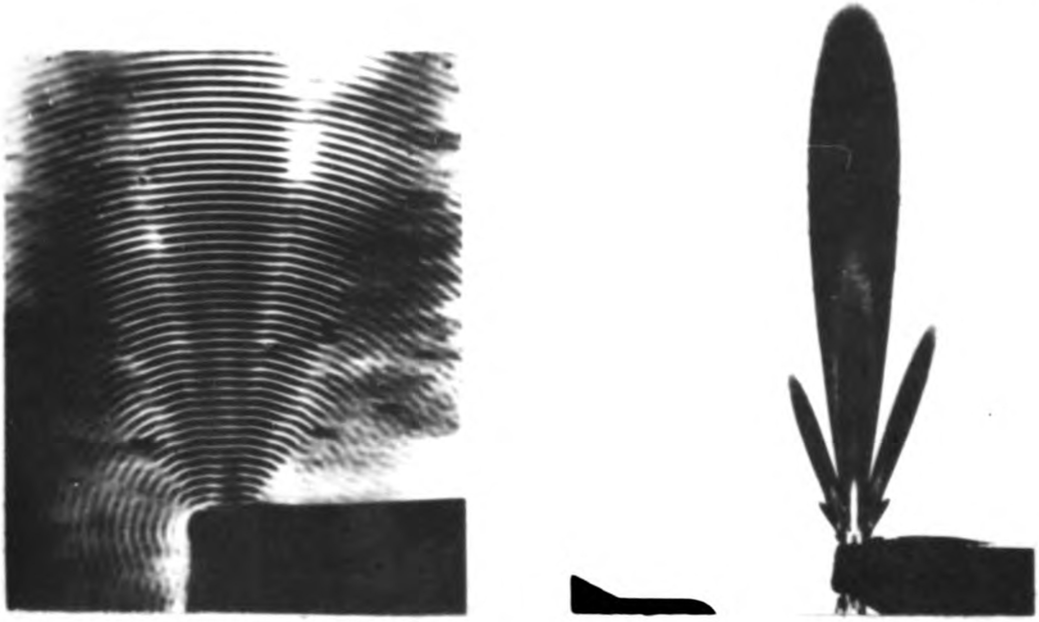

a. Stroboscopic picture of wave fronts. D = 4λ.

b. Patterns of lobes. D $\doteq 4.2\lambda$.

Figure 4. Interference Pattern from a Long Thin Source.

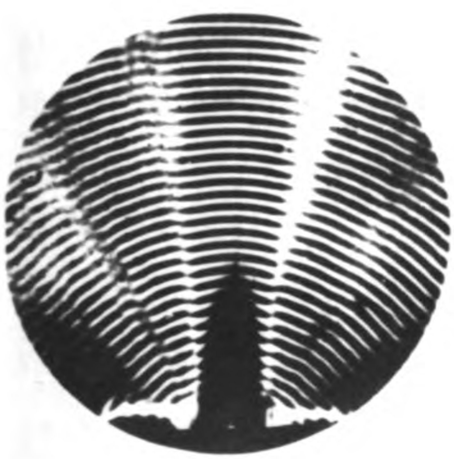

Figure 5. Stroboscopic Picture of Interference Pattern from a Transducer. D $= 3.4\lambda$.

Figure 6. Interference Pattern Showing Intensity Distribution Close to the Transducer. D = 12.8λ.

for the stroboscopic picture, Figure 4a. This picture shows the features far from the source, as well as the near field. Figure 6, obtained by Osterhammel[30] shows the details close to the source of maximum intensity. From these pictures, one can see the intensity distribution both in the Fresnel and the Fraunhofer regions and how the features change with a change of the ratios D/λ.

The theoretical prediction for an extended beam pattern is illustrated in Figure 7. Much of the beam pattern can be observed at low intensities for certain ratios D/λ in the ripple tank. At higher intensity, the fine structure of the pattern close to the source is made apparent.

Osterhammel analyzed this pattern for Fresnel diffraction graphically. This analysis uses the fact that the interference pattern from a slit can be represented as the superposition of a plane wave emerging from the slit and a cylindrical wave from each end. In Figure 8, the plane and cylindrical waves for a slit of $D/\lambda = 8$ are drawn as thin lines. The solid lines indicate crests and the dotted lines indicate troughs. The combining of all points of the same phase gives two groups of confocal parabolas and a group of confocal hyperbolas, with the edge point of the slit as a common focus. The parabolas arise from superposition of a

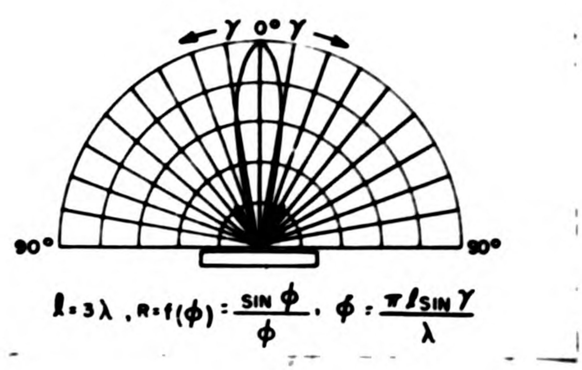

Figure 7. Directional Characteristics of a Rectangular Radiating Surface.

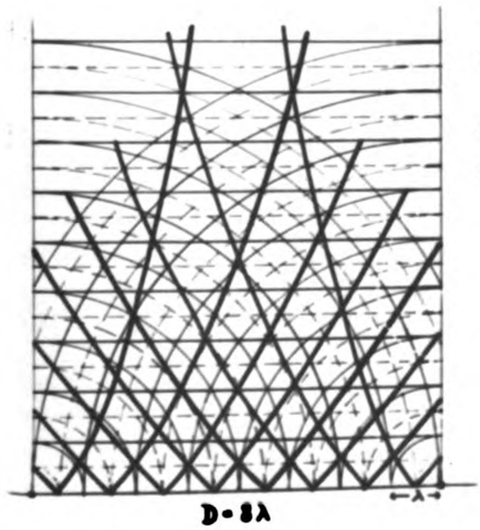

Figure 8. Interaction of Cylindrical Waves from Ends and Plane Waves from the Face of a Transducer. D = 8 λ.

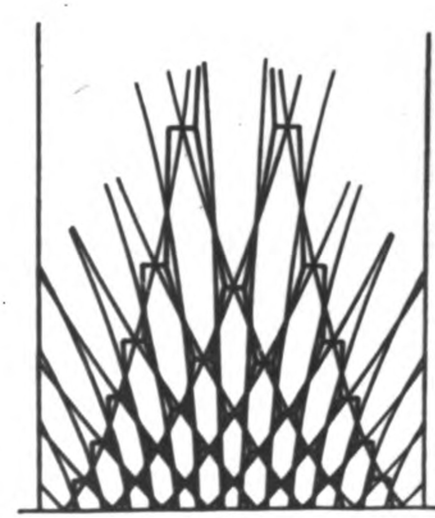

Figure 9. Schematic Drawing of the Interference Pattern Immediately Before a Transducer Showing Intensity Distribution.

plane wave and a cylindrical wave, while the hyperbolas are the superposition of the two cylindrical waves. In Figure 8, the parabolas are the parabolas of minimum intensity. For the complete intensity pattern, both the parabolas and hyperbolas for minimum intensity are plotted in Figure 9. The patterns agree well with experimental results. However, one may get a nearly perfect agreement, if one makes the drawing so that the plane wave is 180° out of phase with the cylindrical waves. Osterhammel had assumed zero phase difference. Gessert and Hiedemann[31], considering the actual form of vibration of quartz, investigated the detail of phase difference and obtained proof for its presence. For surface waves excited by a dipper, both plane and cylindrical waves are in phase.

The ratio of D/λ for the experimental results with the ripple tank must be known in order to make a comparison with the experimental and theoretical results for sound. Two methods were used to obtain this ratio, with the results agreeing very closely.

The simplest method is to measure D and λ directly from the pictures. In order to find D, it is necessary to find the edge of the dipper which is obscured by the meniscus. Since the circular wave fronts at the ends of the dipper originate at the edge, their common center is the edge of the dipper. D is then determined with dividers, and the dividers placed on a portion of the picture where the wave fronts can be counted. This gives a good value for the number of wave lengths in the distance D.

The second method necessitates obtaining the actual value of λ from the frequency and comparing this with the measured value of D for the dipper. In order to determine λ from the frequency, plots (Figure 10) were made of frequency versus wave length for perfectly clean mercury and for very dirty mercury from Equation (1), using values of σ for clean and for dirty mercury, given by Vincent. Then a series of stroboscopic pictures were made from a plane dipper at known frequencies. The magnification of the pictures was determined by photographing a scale in the plane of the waves. The wave length was then obtained directly from the film and plotted on the graph. The experimental curve falls between the extreme theoretical curves, indicating that the surface tension of the mercury used was affected by contamination, but that the contamination was less than the extreme conditions encountered by Vincent. Since the frequency is always known, the wave length is easily obtained. The values of D/λ obtained by this method were in agreement with the values obtained by the other method.

Knowing the ratios of D/λ, comparison can readily

Fig. 10. Wave Length for Sinusoidal Frequencies on a Mercury Surface

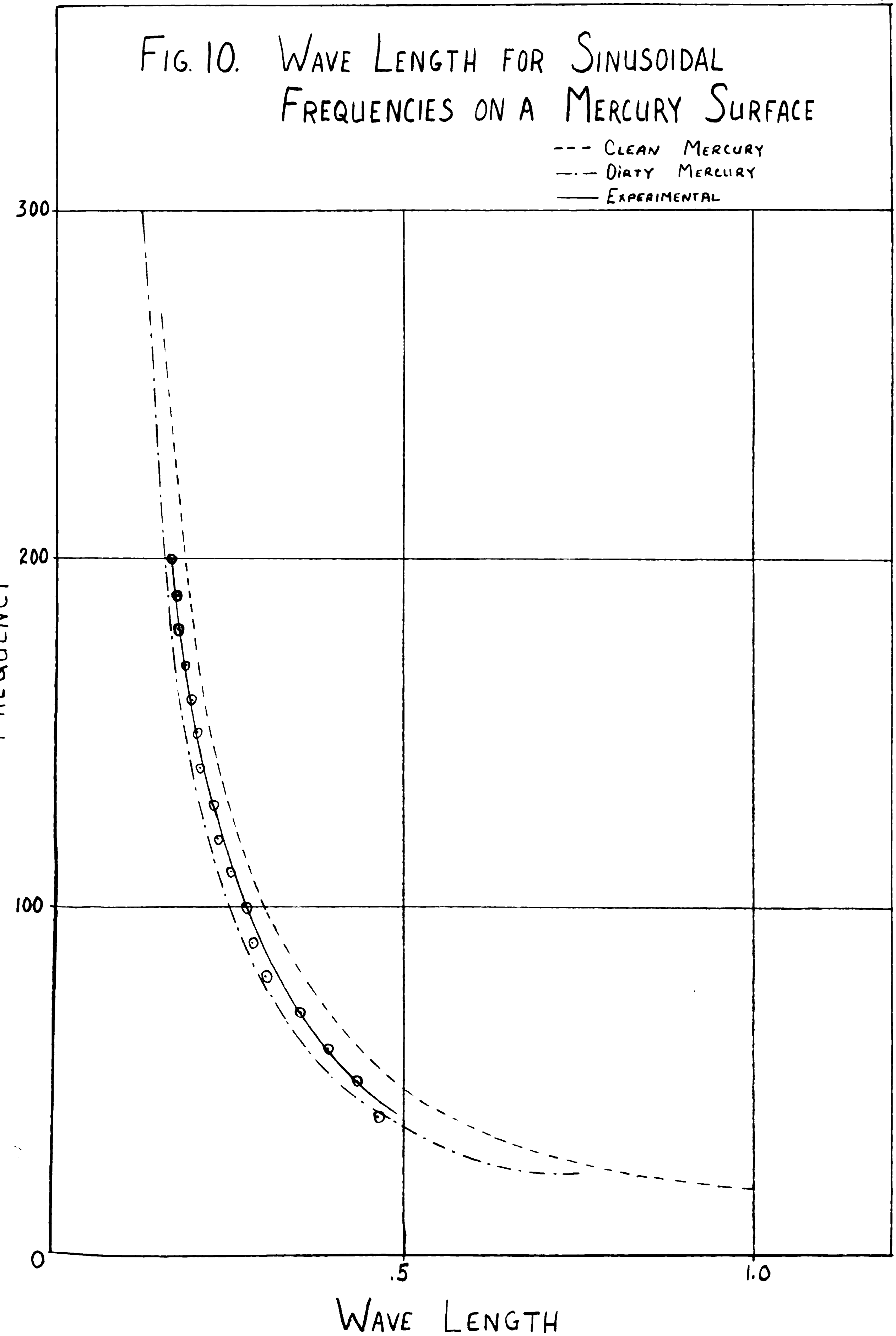

be made between pictures obtained from surface waves and the pictures for sound. In all cases, the stroboscopic picture is (a) and the time average of the intensity is (b). The usual Schlieren method was used for both pictures. Figures 11 and 12 show that the number of lobes is larger as D/λ increases from 2.7 to 6, although the field of view is not large enough to show all lobes. Since all the pictures presented here are in order of increasing D/λ, this can be observed in progressing through this series of pictures. The details of the picture close to the transducer, and how they become more complex, can be observed in Figures 13 and 14 for D/λ changing from 7 to 9. The subsequent pictures illustrate this point for higher ratios.

Increasing the amplitude of vibration of the dipper produces interesting effects. In Figure 15 is given a pattern for a D/λ of 19 at low amplitude; in Figure 16 is the same situation at high amplitude. The differences between these pictures near the dipper can be explained by the effect of the meniscus, which is to obscure part of the pattern at low amplitudes. The similarity between the pattern near the dipper in Figure 16a and the corresponding pattern in Figure 6 is also noteworthy.

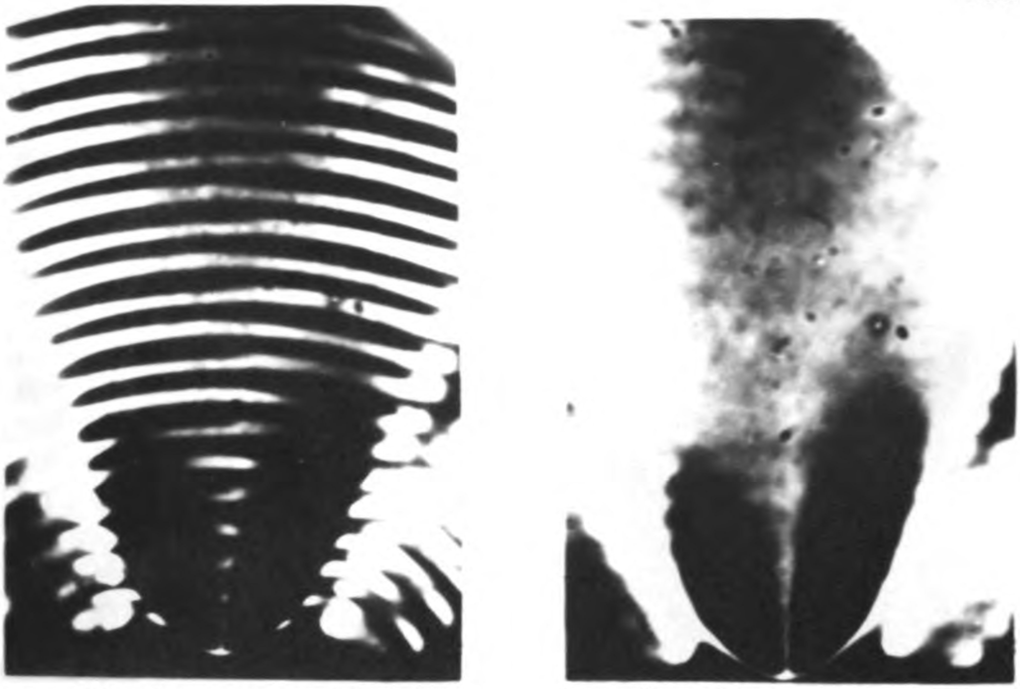

a. Stroboscopic light. b. Continuous light.

<u>Figure 11</u>. Beam Pattern from a 1 cm Transducer at 53$\sim$. $D = 2.7\lambda$.

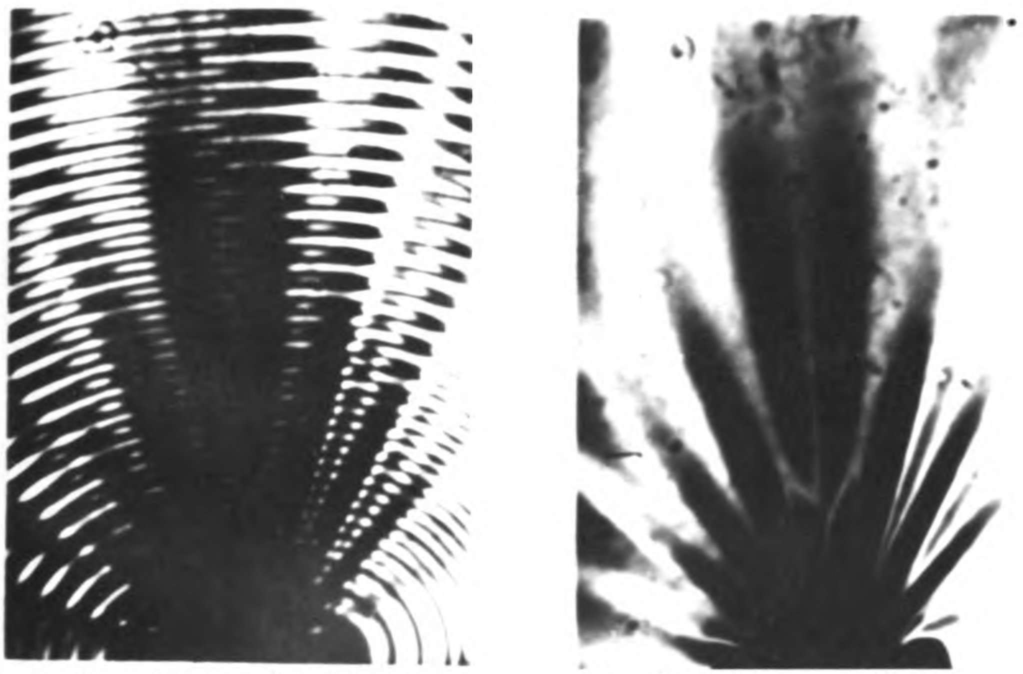

a. Stroboscopic light. b. Continuous light.

<u>Figure 12</u>. Beam Pattern from a 1 cm Transducer at 200$\sim$. $D = 6\lambda$.

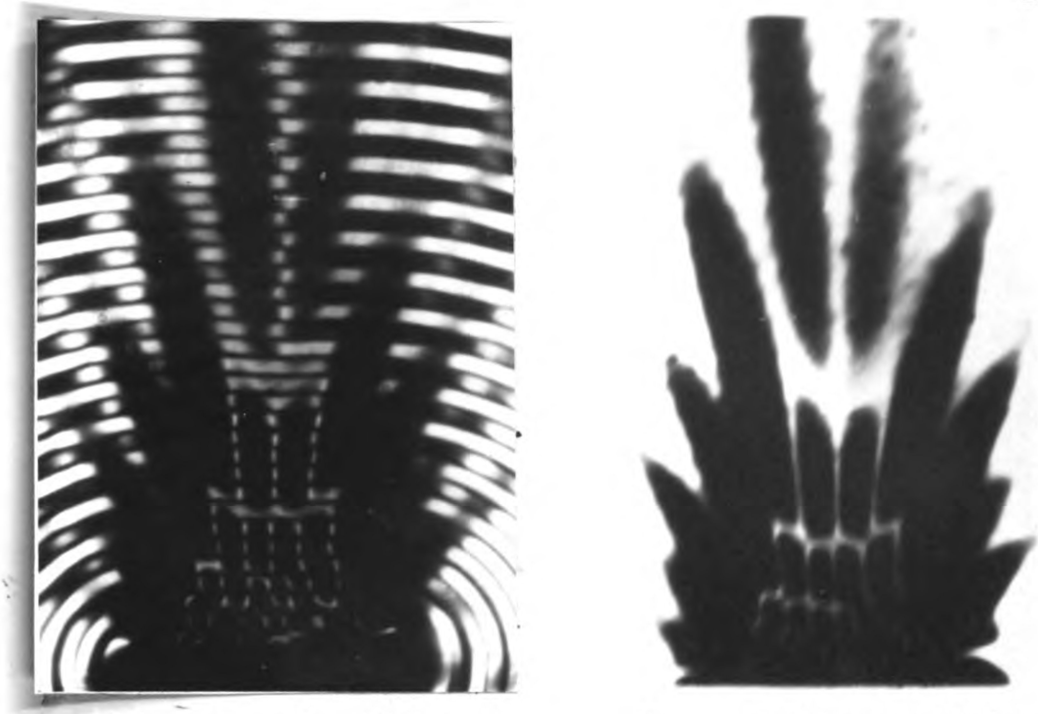

a. Stroboscopic light. b. Continuous light.

Figure 13. Beam Pattern from a 1.5 cm Transducer at 119~. D = 7λ.

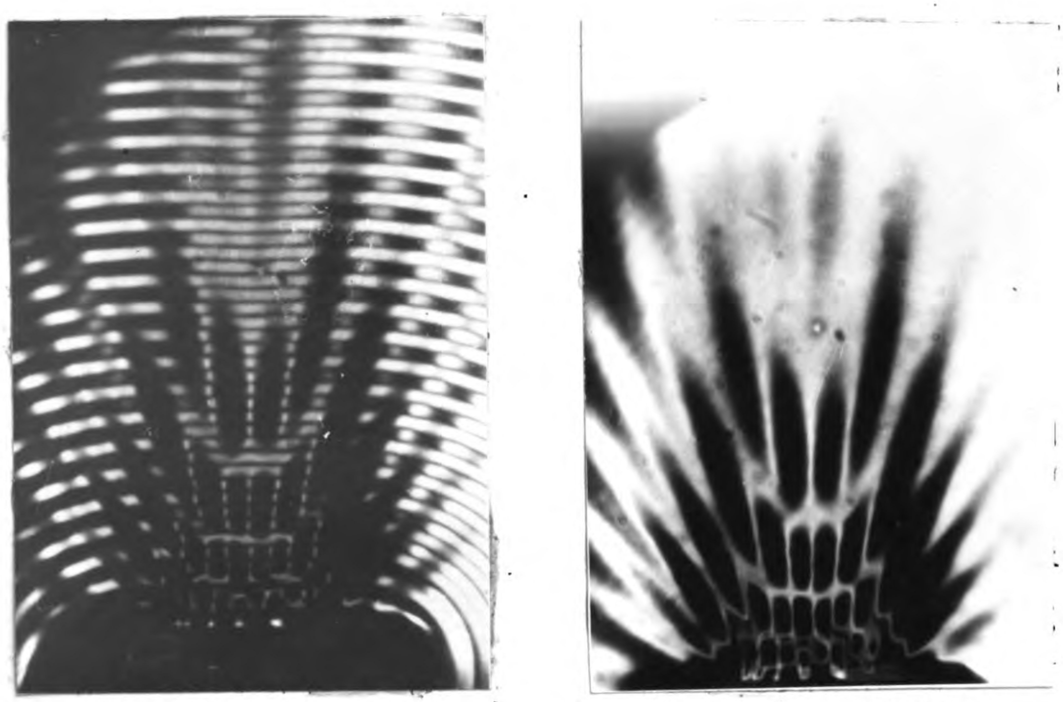

a. Stroboscopic light. b. Continuous light.

Figure 14. Beam Pattern from a 1.5 cm Transducer at 187~. D = 9λ.

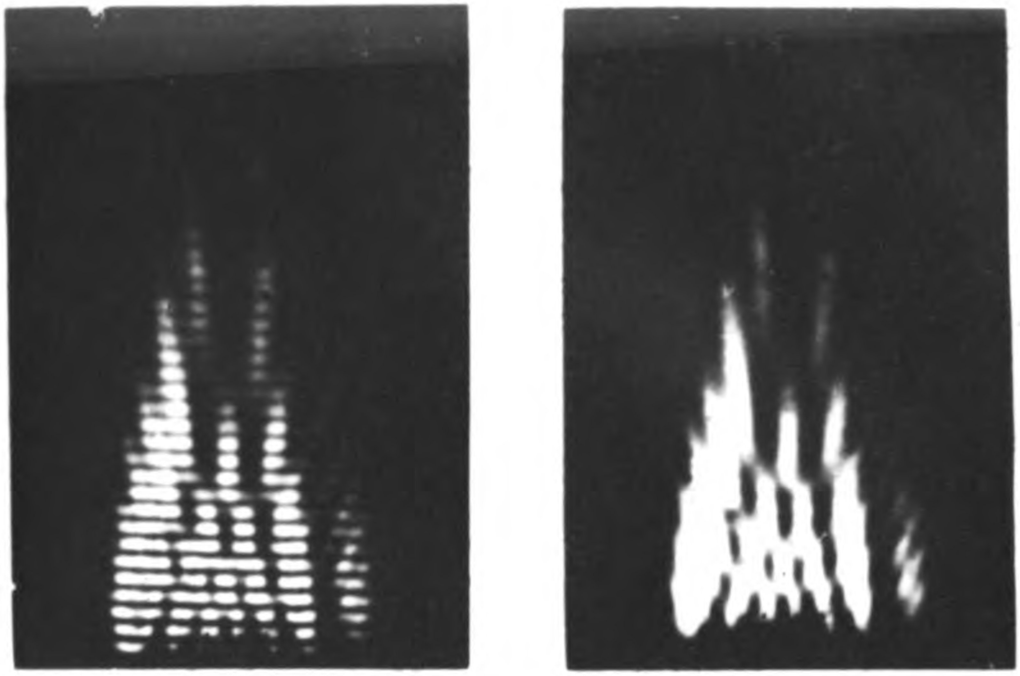

a. Stroboscopic light. b. Continuous light.

<u>Figure 15</u>. Beam Pattern from a 2 cm Transducer at 375~ With the Intensity of the Amplifier Very Low. D = 19λ.

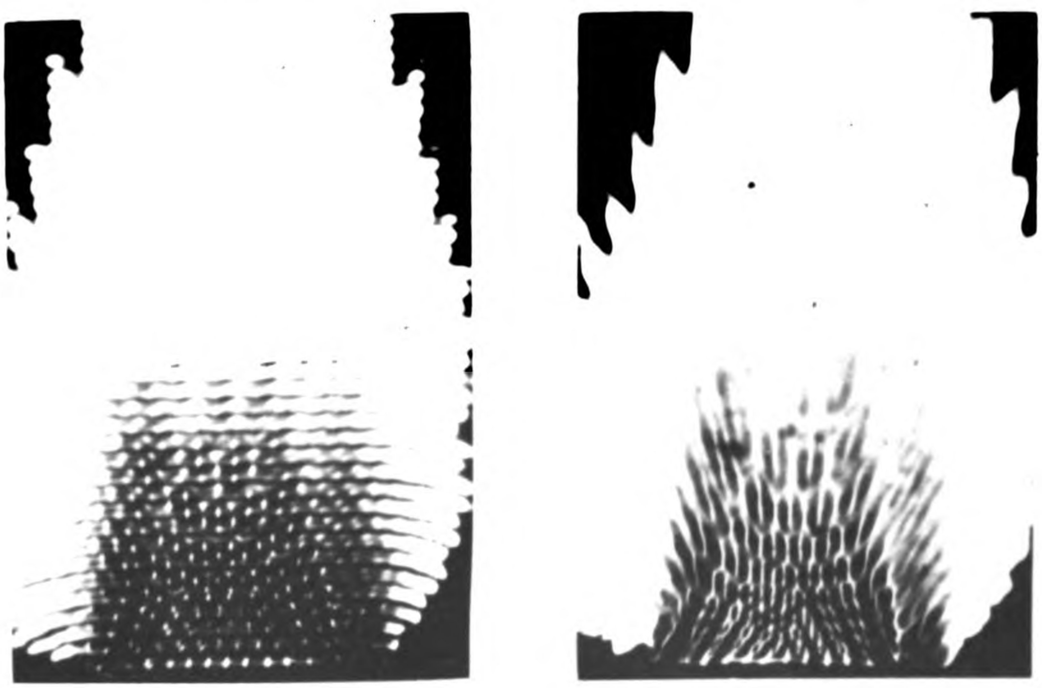

a. Stroboscopic light. b. Continuous light.

<u>Figure 16</u>. Beam Pattern from a 2 cm Transducer at 375~ With the Intensity of the Amplifier High. D = 19λ.

IV. PERIODIC CHANGE OF PHASE TO AMPLITUDE MODULATION

If a ruled optical grating is illuminated with parallel light and the interference phenomena immediately behind the grating are observed on a screen or, in the case of fine gratings, by a microscope, real images may be seen at periodic intervals. These images are bright lines parallel to the grating elements. They are amplitude modulations of the light wave fronts. The sharpness of the lines shows that this modulation is far from sinusoidal. Between these amplitude modulations, there are phase modulations of the wave front. However, in the optical case, this phase modulation cannot be observed. For this reason, one must use analogies to demonstrate the phase modulation. Nomoto[32] diffracted ultrasonic waves with a solid grating and, using a stroboscopic light source, observed the way in which waves interfered. His pictures indicate the periodic change between the amplitude modulation and phase modulation of the ultrasonic wave fronts. This phenomenon in surface waves can be easily observed by the use of a ripple tank. A distinct advantage of this method is that one can produce the interference patterns by both amplitude gratings and phase gratings. Analogous to an amplitude grating is a row of point sources on the liquid surface. This was demonstrated by Vincent[3] for a plane grating and a Rowland grating. This may be obtained by using a dipper which resembles a comb (Figure 3b). The phase grating (Figures 3c and 3d) is a corrugated strip of metal strong enough to avoid flexural vibrations.

Since there is a periodic change between phase and amplitude modulation in the wave interference, one would expect the interference phenomena produced by either an amplitude grating or a phase grating to be very similar. This is confirmed in optics by the fact that the diffraction pattern produced by an amplitude grating is the same as that produced by a phase grating. Figures 17, 18 and 19 confirm this fact for surface waves. In each case, (a) is the picture of the waves generated by the phase grating analogy and (b) is the picture of the waves generated by the amplitude grating analogy. The similarities are obvious.

The length of a period, defined as the distance between identical amplitude modulated waves, is given approximately by $B = 2D/\lambda$, where D is the grating spacing and λ is the wave length. For $D/\lambda >> 1$, higher order terms can be neglected. This relationship was pointed out by Lord Rayleigh[33] for ruled optical gratings. Nath[34], Nomoto[35] and Pisharoty[36] independently derived the same expression for the case of the ultrasonic grating, provided we interpret D to be the wave length of

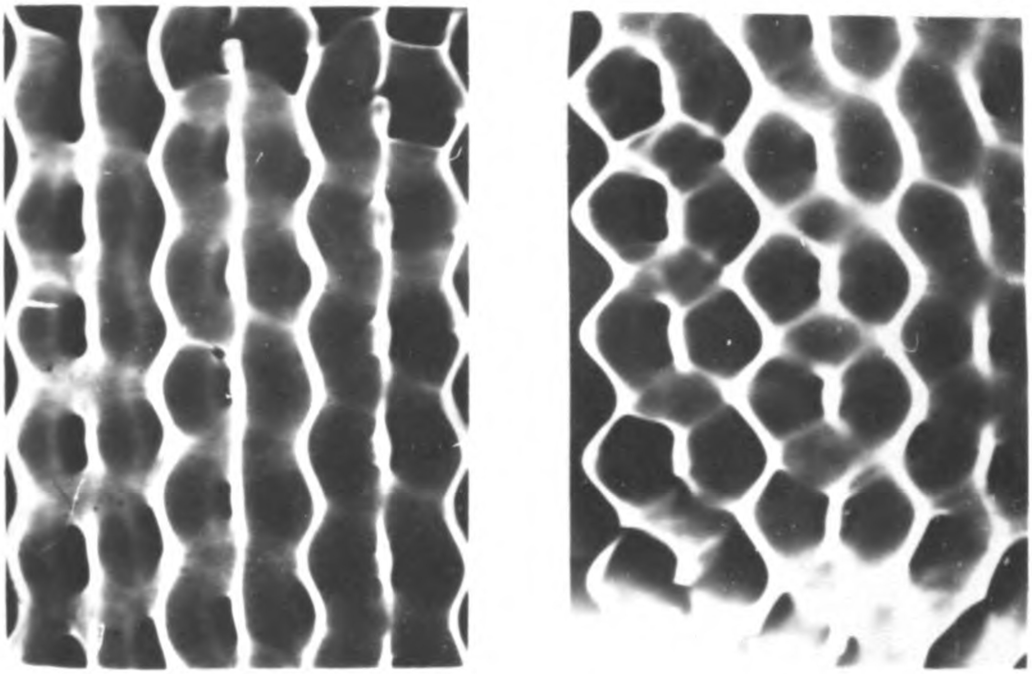

a. Corrugated dipper (phase grating) f = 49.2$\sim$. b. Comb dipper (Amplitude grating) f = 46.5$\sim$.

Figure 17. Interference Pattern Produced by Gratings.

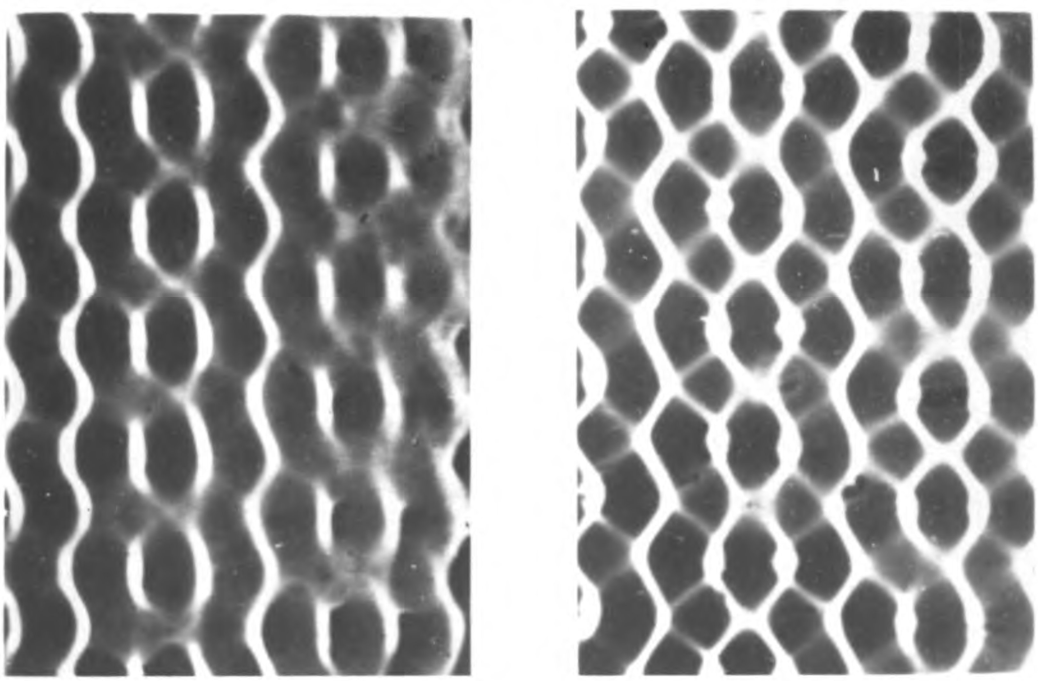

a. Corrugated dipper (phase grating) f = 59$\sim$. b. Comb dipper (Amplitude grating) f = 75$\sim$.

Figure 18. Interference Pattern Produced by Gratings.

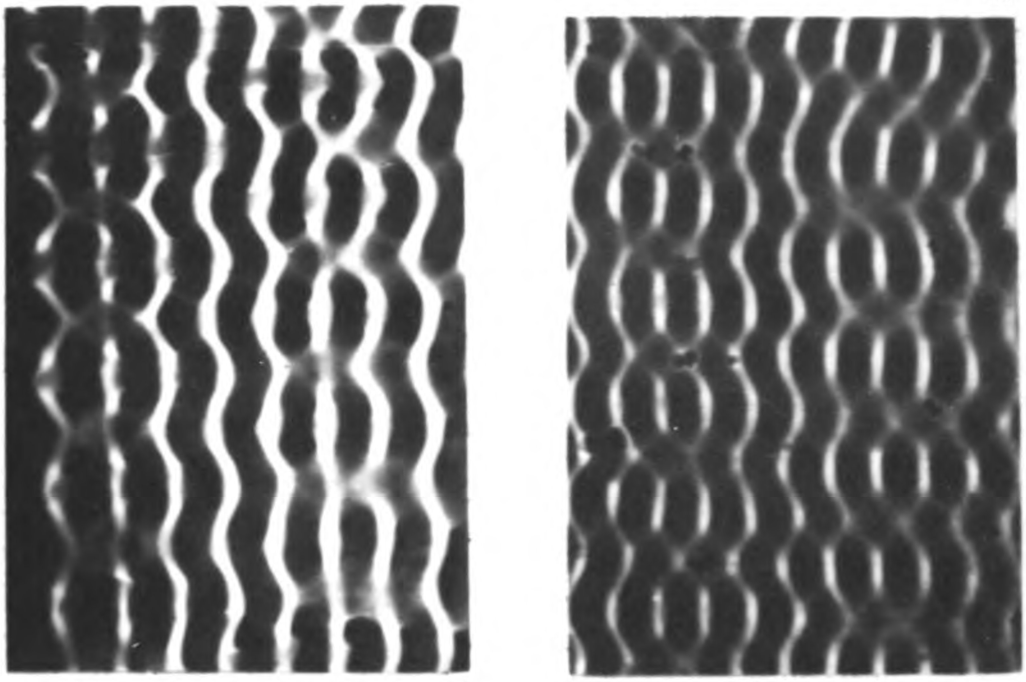

a. Corrugated dipper (phase grating) $f = 79\sim$.

b. Comb dipper (Amplitude grating) $f = 107.5\sim$.

<u>Figure 19</u>. Interference Pattern Produced by Gratings.

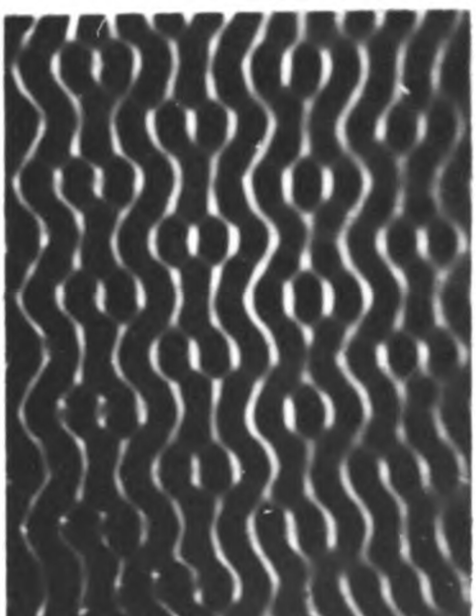

<u>Figure 20</u>. Interference Pattern for Corrugated Dipper. $f = 140\sim$. D/λ is higher.

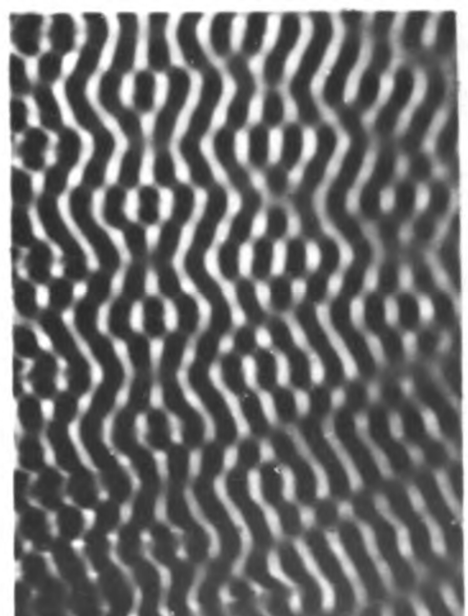

<u>Figure 21</u>. Interference Pattern for Corrugated Dipper. $f = 170\sim$. D/λ is higher.

ultra sound. The equivalence of diffraction of light by a ruled grating and by an ultrasonic grating was demonstrated by Hiedemann and Schreuer[37].

This expression can be used to predict approximately the values of D and λ for the simplest case of a phase modulated wave front followed by an amplitude modulated wave front with no waves between. This condition is satisfied roughly by $B = 4\lambda$ or $D = \sqrt{2}\,\lambda$. A picture of this situation is shown in Figure 17 for both the phase grating and the amplitude grating.

Figures 18 and 19 show the increasing complexities of the patterns with increasing D/λ, accomplished in this case by increasing the frequency. Figures 20 and 21 are patterns for the phase grating analogy at still higher frequencies.

Simple ruled optical gratings can, in first approximation, be regarded as an array of line sources. Each line produces a cylindrical wave. The phase modulation produced by such gratings is therefore similar to a sinusoidal one. This is the reason why the patterns produced by a comb are so much like those made with a corrugated dipper.

As a saw-tooth form of phase modulation can be easily produced with capillary waves, the pattern before such a source (Figure 3d) was also studied. Under certain conditions, the pattern is very similar to the pattern from a sinusoidal source. Under other conditions, the shape of the source is repeated. This is illustrated in Figure 22.

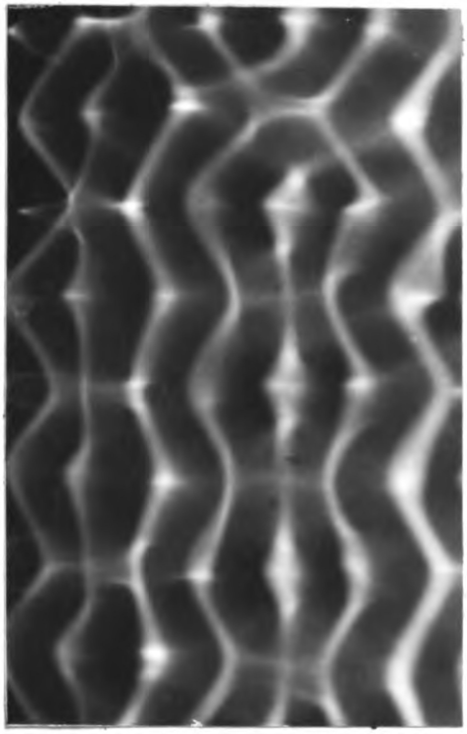

Figure 22. Interference Pattern Produced by a Saw-Tooth Dipper. $f = 44 \sim$.

V. BIBLIOGRAPHY

1. Pohl, R. W., "Physical Principles of Mechanics and Acoustics", Blackie and Sons, London, 1951.

2. Rayleigh, Lord, "On the Tension of Water Surfaces, Clean and Contaminated, Investigated by the Method of Ripples", Phil. Mag. <u>30</u>, 386(1890).

3. Vincent, J. H., "On the Photography of Ripples", Phil. Mag. <u>43</u>, 411(1897).

4. Vincent, J. H., "On the Photography of Ripples, Second Paper", Phil. Mag. <u>45</u>, 191(1898).

5. Vincent, J. H., "On the Photography of Ripples, Third Paper", Phil. Mag. <u>46</u>, 290(1898).

6. Baurand, J., "Etude experimentale des mouvements de l'eau dans un tube et des ondes circulaires produites a la surface de l'eau", Ann. de Phys. (10) <u>18</u>, 107 (1932).

7. Baurand, J., "Propagation d'un train d'ondes periodiques a la surface de l'eau", C. R. (Paris) <u>199</u>, 122(1934).

8. Baurand, J., "Interferences a la surface de l'eau", Journ. Phys. et le Radium (7) <u>7</u>, 365(1936).

9. Bondy, H., "Waves on the Surface of a Compressible Liquid", Proc. Camb. Phil. Soc. <u>43</u>, 75(1947).

10. Brandt, O. and H. Freund, "Gerät Zur Vorführung von Wasserwellen", ZS. f. Unterr. <u>47</u>, 261(1934).

11. Davis, A. H., "Some Acoustical Phenomena Illustrated by Ripple Transmission Through Quincke Filters, Curved Conduits and Vibrating Partitions", Proc. Phys. Soc. <u>40</u>, 90(1928).

12. Davis, A. H., "The Analogy Between Ripples and Acoustical Wave Phenomena", Proc. Phys. Soc. <u>38</u>, 234 (1926).

13. Dean, W. R., "On the Reflection of Surface Waves by a Submerged Circular Cylinder", Proc. Camb. Phil. Soc. <u>44</u>, 483(1948).

14. Kreisel, G., "Surface Waves", Quart. Appl. Math. <u>7</u>, 21 (1949).

15. Longuet-Higgins, M. S., "Mass Transport in Water Waves", Phil. Trans. A, 245, 535(1953).

16. Longuet-Higgins, M. S., "On the Decrease of Velocity with Depth in an Irrotational Water Wave", Proc. Camb. Phil. Soc. 49, 552(1953).

17. Larras, J. and J. Laurent, "Water Waves", C. R. (Paris), 230, 1504(1950).

18. Mercier, R., "Contribution a l'etude des ondes superficielles et interfaciales", Helv. Phys. Acta. 26, 317(1953).

19. Tyler, E., "Experiments with a New Type of Ripple Tank", Proc. Phys. Soc. 48, 659(1936).

20. Van Wieringen, J. S., "Reflection of Light by Rippled Water Surfaces", Proc. K. Ned. Akad. Wet. 50, 952(1947).

21. Yamasaki, K., "On Some Acoustic Experiments Using Water-Waves", Journ. Soc. Mecham, Eng. Japan 35, 772(1932), Phys. Ber. 14, 173(1933).

22. Ursell, F., "Trapping Modes in the Theory of Surface Waves", Proc. Camb. Phil. Soc. 47 (Pt.2), 347(1951).

23. Bouasse, M., "Diffraction des Rides Capillaires", Ann. de Physique 11, 5(1939).

24. Grossmann, E. and E. Hiedemann, "Darstellung der Fresnelschen Beugungserscheinungen mit Wasseroberflachenwellen und Ultraschallwellen", Z. Physik 95, 383(1935).

25. Dorrestein, R., "General Linearized Theory of the Effect of Surface Films on Water Ripples", Proc. K. Ned. Akad. Wet. B 54, 350 (1951).

26. Lamb, Sir Horace, "Hydrodynamics", Dover, New York, 1945, P. 623.

27. Boyle, R. W., J. F. Lehmann and C. D. Reid, "Visualization and Energy Survey of a High Frequency Diffraction Beam", Trans. Roy. Soc. Can. 19, 167(1925).

28. Hiedemann, E., and K. Osterhammel, "Optische Untersuchungen der Richtcharakteristik von Ultraschallquellen", ZS. f. Phys. 107, 273(1937).

29. Hiedemann, E., and K. Osterhammel, "Untersuchung von Schallamplitudenfeldern Mittels einer Methode der Isochromaten", Proc. Indian Acad. (A) 8, 275(1938).

30. Osterhammel, K., "Optische Untersuchung des Schallfeldes Kolbenformig Schwingender Quarze", Akust. ZS. 6, 73(1941).

31. Gessert, W. L. and E. A. Hiedemann, "Ultrasonic Stroboscope for the Study of Ultrasonic Fields", J. Acoust. Soc. Am. 28, 944(1956).

32. Nomoto, Otohiko, "On the Phenomenon of the Periodical Exchange Between Phase-Lattice and the Amplitude-Lattice in the Fresnel's Diffraction Phenomenon by Gratings, Theoretical Considerations and an Experiment by the Ultrasonic Wave", J. Phys. Soc. Japan 2, 41 (1947).

33. Rayleigh, Lord, "On Copying Diffraction-Gratings, and On Some Phenomena Connected Therewith", Phil. Mag. 11, 196(1881).

34. Nath, N. S. N., "The Visibility of Ultrasonic Waves and Its Periodic Vibrations", Proc. Ind. Acad. Sci. 4, 262(1936).

35. Nomoto, O., "Über eine neue Sichtharmachungsmethode stehender Ultraschallwellen in Flussigkeiten", Proc. Phys-Math. Soc. Japan, 18, 402(1936).

36. Pisharoty, P. R., "On the Visibility of Ultrasonic Waves", Proc. Ind. Acad. Sci. 4, 27(1936).

37. Hiedemann, E. and E. Schreuer, "Zur Periodizitat der Abbildung von Ultraschallwellen", ZS. f. Physik 107, 463(1937).